DOI: 10.1002/chem.201002498

Convenient and Efficient FRET Platform Featuring a Rigid Biphenyl Spacer between Rhodamine and BODIPY: Transformation of 'Turn-On' Sensors into Ratiometric Ones with Dual Emission**

Haibo Yu,[a] Yi Xiao,*[a] Haiying Guo,[a] and Xuhong Qian*[b]

Abstract: We have connected a borondipyrromethene (BODIPY) donor to the 5′ position of a tetramethylrhodamine (TMR) acceptor to form a high efficiency (over 99%) intramolecular fluorescence resonance energy transfer (FRET) cassette, BODIPY–rhodamine platform (BRP). While the good spectral overlap between the emission of BODIPY and the absorption of TMR was one favorable factor, another feature of this FRET system was the rigid and short biphenyl spacer that favored efficient through-bond energy transfer. More importantly, in this system, the 2′-carboxyl group of the rhodamine unit was preserved for the further modifications, which was as convenient as those carbonyl groups on the original rhodamines without connection to donors. For this reason, BRP is clearly differentiated from the previous ratiometric sensors based on donor rhodamine systems. To illustrate its value as a versatile platform, we introduced typical Hg^{2+} receptors into BRP, through convenient one-pot reactions on the 2′-carboxyl group, and successfully developed two ratiometric sensors, BRP-1 and BRP-2, with different spirocyclic receptors that recognized Hg^{2+} on different reaction mechanisms. Upon excitation at a single wavelength (488 nm), at which only BODIPY absorbed, both of the FRET sensors exhibited clear Hg^{2+}-induced changes in the intensity ratio of the two strong emission bands of BODIPY and rhodamine. It should be noted that these ratiometric Hg^{2+} sensors exhibited excellent sensitivity and selectivity Hg^{2+}, as well as pH insensitivity, which was similar to the corresponding 'turn-on' rhodamine sensors. While both ratiometric probes were applicable for Hg^{2+} imaging in living cells, BRP-1 exhibited higher sensitivity and faster responses than BRP-2. Our investigation indicated that on a versatile platform, such as BRP, a large number of highly efficient ratiometric sensors for transition-metal ions could be conveniently developed.

Keywords: donor–acceptor systems · fluorescence · FRET · mercury · sensors

Introduction

Owing to the important roles of transition- and heavy-metal cations in the areas of biological, environmental, and chemical systems,[1,2] the development of new chemosensors for these cations has been of interest.[3] Particularly, in recent decades, there has been a considerable increase in fluorescent sensors research, because of their advantages in optical signal outputs, cell penetrability, and noninvasive imaging of cells in vivo.[4] As transition- and heavy-metal ions often act as efficient fluorescence quenchers, 'turn-off' sensors are common.[5] However, because of their low signal-to-noise ratio, turn-off sensors are less sensitive than the 'turn-on' ones.[6] Thus, intensive efforts have been directed toward the development of turn-on fluorescent sensors, which have become mainstream.[7] Among various strategies, the chemodosimeter approach[8] provides good opportunities to design turn-on sensors for transition-metal ions with both high sensitivity and selectivity.

Recently, rhodamine spirolactams, as novel chemodosimeters, have attracted much attention and have been widely utilized in the design of turn-on sensors.[9] The turn-on response to certain transition cations have involved ring-opening transformations from colorless and nonfluorescent spirocyclic forms to rhodamine fluorophores with intensive absorptions and emissions in the visible spectrum range (Scheme 1). The remarkable fluorescence enhancements ensure the high signal-to-noise ratios of such sensors. More importantly, by introducing specially designed receptors to the spirolactam's imide site, high reactivity and selectivity toward a specific metal cation can be achieved. So far, efficient rhodamine spirolactam sensors for various transition-

[a] H. Yu, Prof. Dr. Y. Xiao, H. Guo
State Key Laboratory of Fine Chemicals
Dalian University of Technology, Zhongshan Road 158
Dalian, 116012 (P.R. China)
Fax: (+86) 411-83673488
E-mail: xiaoyi@dlut.edu.cn

[b] Prof. Dr. X. Qian
Laboratory of Chemical Biology
East China University of Science and Technology
Meilong Road 130, Shanghai, 200237 (P.R. China)
Fax: (+86) 21-64252603
E-mail: xhqian@ecust.edu.cn

[**] BODIPY = borondipyrromethene.

Supporting information for this article is available on the WWW under http://dx.doi.org/10.1002/chem.201002498.

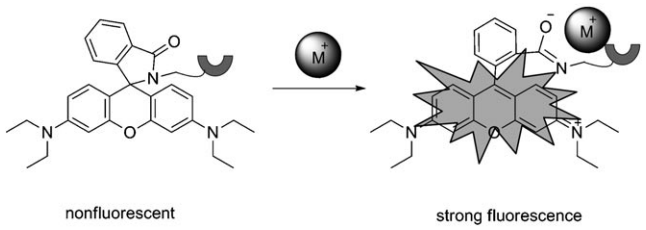

Scheme 1. Ring-opening reaction of rhodamine fluorophores used in the design of turn-on sensors.

and heavy-metal cations, such as Cu^{2+},[10] Hg^{2+},[11] Fe^{3+},[12] Cr^{3+},[13] Au^{3+},[14] Pb^{2+},[15] and Ag^{+},[16] have been successfully developed. Moreover, such a rhodamine spirolactam chemodosimeter strategy has also been extended to sensing active oxygen species[17] and amino acids.[18] For convenient chemical modification on the spirolactam imide (carboxyl group), conventional rhodamine dyes have become versatile platforms to design turn-on sensors. Their applications are important in the field of fluorescent sensors, as indicated by the large amount of recent publications on this topic.

Although the significant fluorescence enhancement contributes to cell identification in tissue imaging, turn-on sensors have an intrinsic limitation. Because, for these single-emission sensors, the accuracy of quantitative detection might be limited by factors such as fluctuating intensities of the excitation light, the concentration of the fluorescent sensor, inner filter effects, or something as trivial as variation in the distance between the sample and the excitation light or detector.[19] To solve this problem, some work has focused on the design of ratiometric sensors. These sensors utilized the ratios of emission intensity at two different wavelengths as signal outputs, which, in principle, or ideally, should be capable of self-calibration and independent of both excitation light and sample concentration. An intramolecular charge-transfer (ICT) mechanism is frequently adopted to develop ratiometric sensors, the emission bands of which shift upon binding a guest.[20] However, before and after binding the target ions, the maximum excitation wavelength changes remarkably, and there are large overlaps between the two emission bands owing to the broad fluorescence spectra of ICT fluorophores. These two aspects make it difficult for ICT sensors to accurately determine the ratio of the two fluorescence peaks. Theoretically, the above problems can be avoided by using a FRET-based sensor for which the single excitation wavelength of the donor fluorophore releases the acceptor emission at a longer wavelength.[21]

Since 2008, a novel strategy of connecting a shorter-wavelength fluorophore to a rhodamine spirolactam has brought about several ratiometric sensors for metal cations (Scheme 2).[22–26] The idea is a combination of the chemodosimeter approach and a FRET mechanism. Initially, a rhodamine spirolactam unit with a nonconjugated structure, which has no absorption in the visible range and cannot act as energy acceptor, due to the poor spectral overlap, cannot undergo a FRET process. A ring-opening reaction induced by metal ions generates intensively colored rhodamine dye, which is a good energy acceptor, and thus the FRET process is switched on. This strategy is the so-called spectral overlap-modulated FRET process. The successful examples given in Scheme 2 reveal that the construction of a FRET cassette by attaching a donor fluorophore to rhodamine is highly feasible to transform turn-on sensors into ratiometric ones. However, unexpectedly, this strategy has not been widely applied, and rhodamine-derived ratiometric sensors for metal cations are rare, in contrast to the situation in which large numbers of turn-on rhodamine sensors have been reported frequently in recent years.

When we attempted to analyze why the extension of such a promising strategy has been hampered, we concluded that the lack of a versatile FRET platform was the major reason. As can be foreseen from the structures in Scheme 2, to synthesize these compounds, chemists will be forced to use an

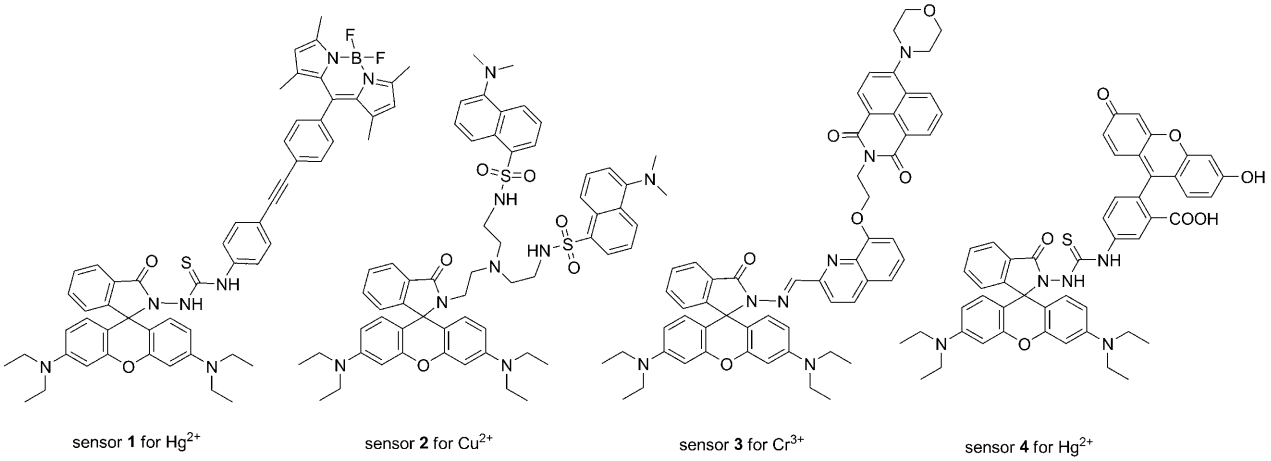

Scheme 2. Representative FRET ratiometric sensors for different metal ions based on a rhodamine fluorophore.

individual and long synthetic pathway for each compound. If there is a ready FRET platform on which convenient modifications result in a large number of ratiometric sensors specific for various analytes, synthetic procedures will be simplified to large extent. We decided to take on the challenging task of constructing an efficient and versatile FRET platform, BRP, to provide the opportunities to develop many ratiometric sensors in a simplified method, by borrowing the experiences accumulated in the development of turn-on rhodamine sensors. With BRP as a precursor, we successfully developed two ratiometric sensors, BRP-1 and BRP-2, conveniently by introducing two different and known Hg^{2+} receptors, and their excellent Hg^{2+} ratiometric responses justified our idea.

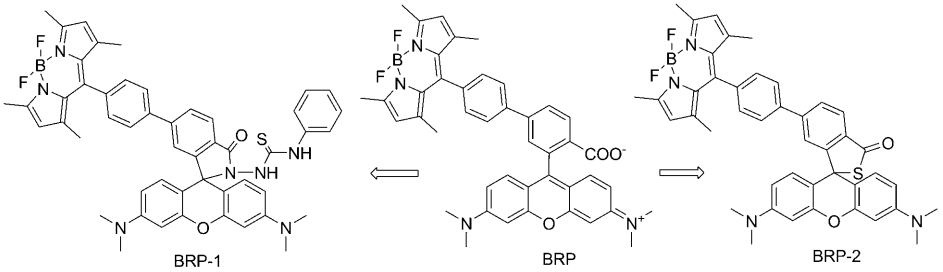

Results and Discussion

Considerations in the construction of the BRP platform: BRP, with a borondipyrromethene (BODIPY) donor connected to a tetramethylrhodamine (TMR) acceptor, is an intramolecular FRET cassette. BRP could be regarded as a versatile platform because the 2′-carboxyl group of the rhodamine unit was preserved for further modifications. This carboxyl group in the BRP structure maintained a similar reactivity to those of ordinary rhodamine dyes without connected donors. As is known, the 2′-carboxyl group of the rhodamine dyes readily condenses with various amino-containing receptors to produce spirolactam-type turn-on sensors for several transition-metal cations. Clearly, all of these known receptors, and those developed in the future, could be introduced into BRP under similar conditions. The difference is that spirocyclic sensors built on BRP will be ratiometric ones based on the FRET mechanism. With BRP as a platform, and by using knowledge of rhodamine turn-on sensors, the originally difficult task to search for ratiometric sensors is considerably simplified, only the facile installation of ready-made components is required. To the best of our knowledge, there has been no BRP-like versatile platform for ratiometric sensors of metal cations, although rhodamine dyes have been adopted as acceptors in some FRET systems that have been designed for other applications. Incidentally, another important and unique feature of BRP is that the spirocyclic receptors induced on the remaining 2′-carboxyl group can recognize the corresponding cations without influence from/to other parts of the molecule (spacer or donor) for their separation from each other. For the previous ratiometric rhodamine sensors **1**–**4**, the receptors were introduced between the rhodamine and donors, so they were integral parts of the spacers. The spatial proximity of the reactive recognition site to other bulky groups might lower the sensitivity or selectivity toward the analytes, relative to those of the original turn-on rhodamine sensors.

In our design, a short and rigid biphenyl spacer was adopted to satisfy the requirements for consistent and highly efficient energy transfer. First, the short and rigid biphenyl group ruled out the inaccuracy caused by changes in the distance and orientation between the donor and the acceptor. Because in FRET systems with flexible and relatively long spacers, these changes would be likely to happen dynamically in the inhomogeneous biological microenvironment,[27] and then affect the energy-transfer efficiency.[28,29] Although sensitivities in distance/orientation were very useful design features for sensors monitoring conformational or functional changes in biological macromolecules, such as DNA beacons and enzyme activity sensors,[30] unfortunately they interfere unfavorably for sensing small molecular analytes in local microenvironments. Second, a short, rigid biphenyl spacer with a partly conjugated nature was good for high-efficiency FRET through bonds. Excellent work by the group of Burgess and others suggested superfast and efficient energy-transfer systems through bonds with donor and acceptor fragments linked with various rigid spacers.[31] The rigid biphenyl spacer as a twisted, but otherwise conjugated, π-electron system could keep the energy-transfer time on the picosecond scale, which is faster than that of through-space energy transfer.[32]

We preferred to use BODIPY rather than other fluorophores in the construction of a platform for ratiometric sensors. In our understanding of the spectral overlap-modulated FRET strategy, whereas the rhodamine unit should be sensitive to cations, the donor fluorophore should have a strong and stable fluorescence that is insensitive to environmental factors, such as polarity and pH, since the donor would simultaneously act as the internal standard for ratiometric detection. BODIPY fulfills this requirement and should be superior to other donors, such as dansyl amide, naphthalimide, and fluorescein, adopted in previous ratiometric FRET sensors, for example, sensor **2**–**4**. Moreover, the emission band of BODIPY is so narrow that it can be easily separated from the emission band of rhodamine, which is similarly narrow. The distinct dual nonoverlapping fluorescence signals of BODIPY-rhodamine systems are highly desirable in the process of ratio measurement. Although BODIPY is very popular in FRET investigations,[33] its good match to

rhodamine has only been revealed recently.[22,34] This excellent FRET pair has not yet been extensively studied.

Synthesis of the BRP platform and BRP-1 and BRP-2 sensors: The synthesis of the BRP platform is shown in Scheme 3. The compounds 4′-B-BODIPY and 5′-Br-TMR were prepared according literature procedures.[35] BRP was efficiently and straightforwardly obtained by the Suzuki coupling of 4′-B-BODIPY and 5′-Br-TMR catalyzed by $Pd(OAc)_2$ in the presence of PPh_3 and Na_2CO_3. The target product BRP was easily obtained and isolated in 78% yield after purification by column chromatography. The BODIPY moiety was connected to the 5′ position of TMR, and the 2′-carboxyl group was preserved in BRP. This rigid connection keeps the orientation of donor and acceptor constant to favor through-bond FRETs.[36]

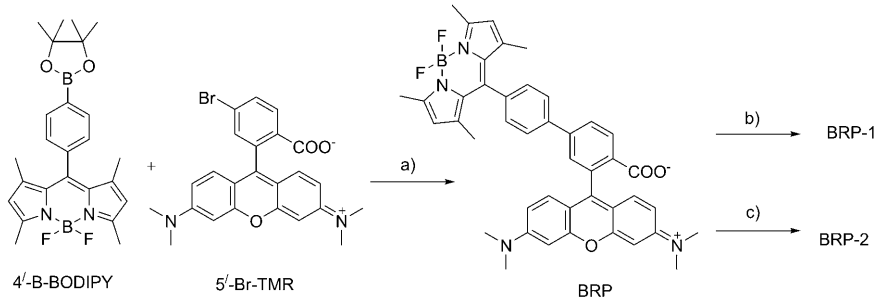

Scheme 3. The synthesis of BRP, BRP-1, and BRP-2: a) $Pd(OAc)_2$, PPh_3, Na_2CO_3, *n*-propanol/methanol; b) 1) NH_2NH_2, CH_3OH; 2) PhNCS, DMF; c) 1) $POCl_3$, $ClCH_2CH_2Cl$; 2) Na_2S, CH_3CN.

To demonstrate BRP as a platform to design ratiometric sensors, two FRET sensors, BRP-1 and BRP-2, were synthesized. BRP-1 and BRP-2 were conveniently obtained according to the synthetic method used in the design of turn-on rhodamine sensors.[37,38] BRP-1 and BRP-2 were prepared in moderate and good yields, respectively, from platform BRP by using two-step procedures. Details of the syntheses are given in the Experimental Section. The convenient synthetic routes of sensors BRP-1 and BRP-2 further indicated that most receptors reported in turn-on rhodamine sensors could be easily introduced into the BRP platform to design ratiometric sensors.

Spectral properties of platform BRP: BRP is not only a precursor or platform, but may also be a sensor or logic gate molecule, since the reversible switching of a rhodamine dye between a zwitterion and a lactone is sensitive to temperature, pH, polarity, proticity, and so forth. As illustrated in Figure 1, BRP switches between the two structures as readily as ordinary rhodamine dyes, which means that, within BRP, energy-transfer processes can be switched off or on. In aprotic solvent, such as acetonitrile, BRP emitted a strong green fluorescence; the fluorescence spectrum showed a single band ($\lambda_{flu}=510$ nm) characteristic for BODIPY. The fluorescence quantum yield of BRP in acetonitrile was 0.43, which was lower than that of 4′-Br-BODIPY ($\Phi=0.61$). There would be photoinduced electron transfers from the spirolactone of rhodamine moiety to the BODIPY fluorophore in the BRP platform, which would result in partial quenching of the fluorescence of BODIPY. This is understandable because the spirolactone form of the rhodamine moiety with amino groups is relatively rich in electron density. In recent work, we found that electron transfer might be an important factor that required careful consideration in the design of FRET systems.[39] A longer-wavelength rhodamine emission band was not detectable, indicating that FRET could not occur. The reason was that the rhodamine

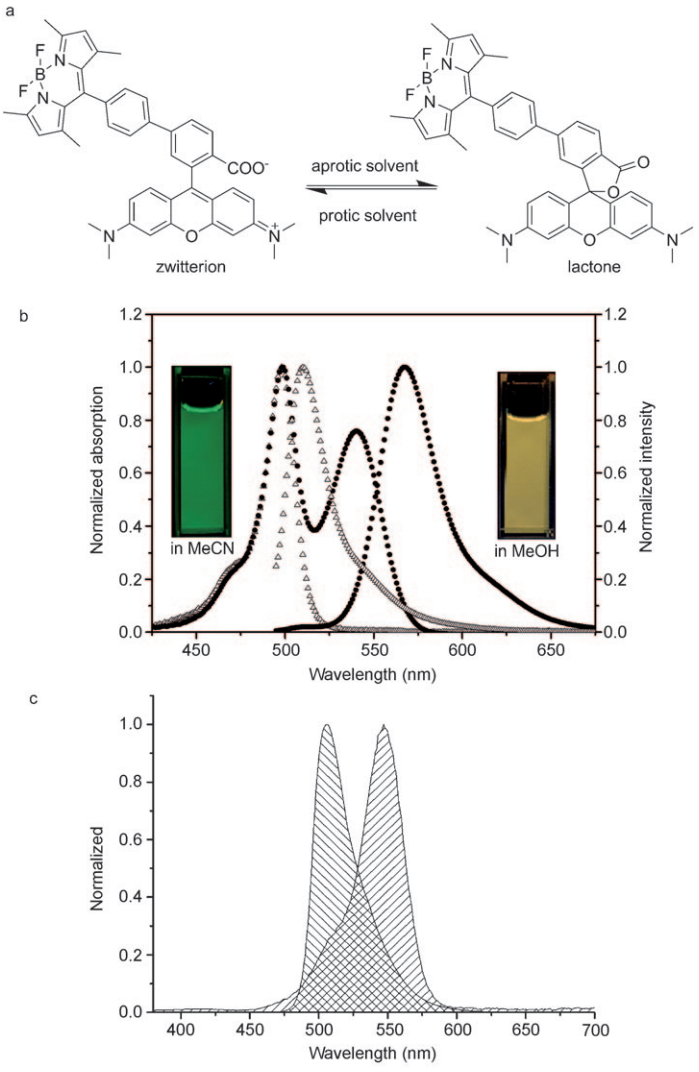

Figure 1. a) The structural changes of BRP between zwitterion and lactone. b) Normalized absorption and emission spectra of BRP in acetonitrile (△) and methanol (●), respectively. c) The overlap between the emission of 4′-Br-BODIPY (left) and the absorption of 5′-Br-TMR (right).

unit was in the spirolactone form, which, without absorption in the visible range, could not act as an acceptor. In protic solvent, such as methanol, BRP emitted a strong orange fluorescence ($\Phi = 0.47$). The fluorescence spectrum showed only a band ($\lambda_{flu} = 568$ nm) characteristic for rhodamine, upon excitation of BODIPY at 488 nm, which indicated that FRET was switched on. The rhodamine unit existed in the form of a ring-opened zwitterion, which had a characteristic absorption peak at 540 nm. It acted as an efficient acceptor, the absorption of which overlapped well with the emission of BODIPY. The overlap integral was also assessed as shown in Figure 1c.

Table 1. Spectral data for 4′-Br-BODIPY, 4′-B-BODIPY, 5′-Br-TMR, and BRP.

Compound	Solvent	λ_{abs} [nm][a]	$\log \varepsilon$[b]	λ_{em} [nm][a]	Φ[c]	η_{EET}[h] [%]
4′-Br-BODIPY	MeCN	498	4.96	514	0.61[d]	–
	MeOH	499	5.00	515	0.54[d]	
4′-B-BODIPY	MeCN	498	4.96	513	0.55[d]	–
	MeOH	498	4.98	513	0.53[d]	
5′-Br-TMR	MeOH	541	5.00	565	0.56[e]	–
BRP	MeCN	498	4.94	510	0.43[d]	–
BRP	MeOH	498	5.14	568	0.47[f]	99
		540	5.02		0.49[g]	

[a] λ_{abs} = absorption maximum; λ_{em} = fluorescence emission maximum. [b] ε = molar extinction coefficient. [c] Φ = fluorescence quantum yield. [d] The quantum yield was determined by using fluorescein as a standard. [e] The quantum yields were determined by using rhodamine 6G as a reference.[42] [f] $\lambda_{ex} = 488$ nm. [g] $\lambda_{ex} = 530$ nm. [h] η_{EET} = the efficiency of energy transfer.

The spectra data of BRP and intermediate compounds are shown in Table 1. The maximum absorption bands of BRP in methanol were at 498 and 540 nm, which corresponded to the absorption of 4′-Br-BODIPY and 5′-Br-TMR, respectively. Upon excitation of BRP at 488 nm, the emission peak was shown at 568 nm owing to FRET and the pseudo-Stokes shift was up to 70 nm. During the process of energy transfer, the spectral properties of the TMR unit were not changed relative to 5′-Br-TMR. The fluorescence quantum yields of BRP ($\Phi = 0.47$, 0.49) in methanol were constant upon excitation at 488 and 540 nm, respectively, which was attributed to through-bond energy transfer from BODIPY to the TMR fluorophore. According to results reported by Burgess et al.,[32] the energy-transfer time in the range of picoseconds and the rigid connection between donor and acceptor were significant characteristics for through-bond energy transfer. The rigid biphenyl group was a critical factor for energy transfer within the BRP platform, which could keep the orientation of donor to acceptor constant to favor through-bond FRET.

The Forster critical radius, R_0 (in Å), was calculated by using Equation (1):

$$R_0 = 0.211[k^2 n^{-4} \Phi_D \int_0^\infty I_D(\lambda)\varepsilon_A(\lambda)\lambda^4 d\lambda]^{1/6} \quad (1)$$

in which k^2 is the orientational factor, Φ_D is the quantum yield of fluorescence emission of the donor, n is the average refractive index of the medium in the wavelength range where spectral overlap is significant, $I_D(\lambda)$ is the normalized fluorescence spectrum of the donor, $\varepsilon_A(\lambda)$ is the molar absorption coefficient of the acceptor (in $dm^3 mol^{-1} cm^{-1}$), and λ is the wavelength in nanometers. As previously reported, the orientation factor was assumed to be equal to the dynamic average that is 2/3. The Forster critical radius of the BRP platform was 20.3 Å. The efficiency of energy transfer (EET) was calculated according to Equation (2):[40]

$$\eta_{EET} = 1 - \Phi_{F(dyad)}/\Phi_{F(donor)} \quad (2)$$

in which η_{EET} is the efficiency of energy transfer, $\Phi_{F(dyad)}$ is the fluorescence quantum yields of the dyad (the donor part in FRET system), and $\Phi_{F(donor)}$ is the fluorescence quantum yields of the donor when not connected to the acceptor. The fluorescence quantum yields ($\Phi_{F(donor)}$) of 4′-Br-BODIPY[41] in methanol was 0.54, whereas that of the BODIPY part in BRP ($\Phi_{F(donor)}$) was greatly reduced to 0.005. Thus, the efficiency of BRP (η_{EET}) in the on state is very high, up to 99%.

The BRP platform exhibited an interesting equilibrium between lactone and zwitterion, which depended on the solvent hydrogen-bond-donating ability and solvent dielectric/polarizability characteristics.[43] Although BRP can respond to many common parameters, such as temperature and pH, the switch could be controlled easily in some specific conditions. Because the switching of ordinary rhodamine dyes has been successfully applied in many fields, such as imprinting,[44] indicators,[45] and molecular sensors,[46] we anticipated that the BRP platform might also be used as a sensor or indicator.

Properties of sensor BRP-1: The mechanism of the reaction between BRP-1 and Hg^{2+} is shown in Scheme 4. The thiosemicarbazides section of BRP-1 was transformed into a 1,3,4-oxadiazide promoted by Hg^{2+}, resulting in the irreversible

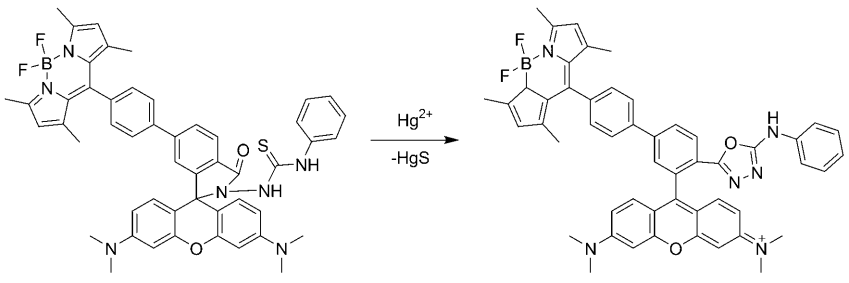

Scheme 4. Hg^{2+}-induced ring opening and cyclization of BRP-1.

ring-opening reaction of the rhodamine section. The product of the reaction between BRP-1 and Hg^{2+} was characterized by ESI-MS analyses (*m*/*z* 824.4310 $C_{50}H_{45}BF_2N_7O^{2+}$; Figure S1 in the Supporting Information). A similar Hg^{2+}-promoted reaction of thiosemicarbazides to form 1,3,4-oxadiazoles was reported previously for a turn-on rhodamine sensor.[37] The absorption and fluorescence titration of Hg^{2+} was conducted by using 0.3 μM BRP-1 in ethanol/water (80/20 v/v) at pH 7.2. In the absence of Hg^{2+} the absorption and emission spectra of BRP-1 only displayed the features of BODIPY. Apparently, the rhodamine spirolactam did not absorb in the visible range and could not accept the energy from BODIPY. Upon the addition of Hg^{2+}, the new absorption band at 562 nm appeared and increased, which indicated that the rhodamine chromophore was generated. Consequently, the large spectral overlap between the emission of BODIPY and the adsorption of rhodamine switched the FRET on.

As shown in Figure 2, with increasing Hg^{2+} concentrations, the BODIPY emission signal at 510 nm decreased, and the rhodamine emission signal at 584 nm appeared and gradually increased in intensity. Upon addition of Hg^{2+} from 0.03–0.15 μM, the emission intensities at 510 and 584 nm were linearly proportional to the amount of Hg^{2+} (Figure S2 in the Supporting Information). However, the ratio of the emission intensities at 584 and 510 nm (I_{584}/I_{510}) was a curvilinear function with the Hg^{2+} concentration over the range of 0.03 to 0.3 μM (6–60 ppb). The Hg^{2+} response range of one order of magnitude was relatively narrow, reflecting the high sensitivity and quantitatively reactive characteristic of the rhodamine spirolactam chemodosimeter.[37] The detection limit of Hg^{2+} is at the parts per billion (ppb) levels. The response to Hg^{2+} was very fast and all spectra were recorded within 5 min after addition of Hg^{2+}.

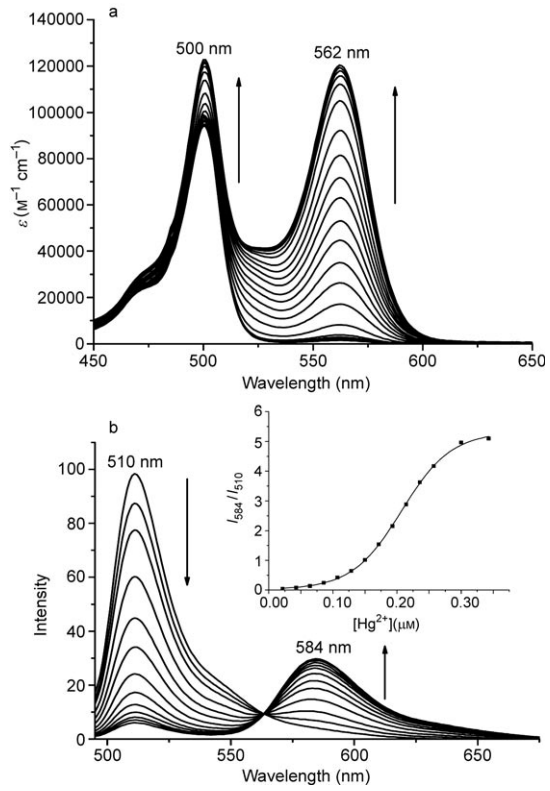

Figure 2. Changes in the absorption (a) and emission spectra (b) of BRP-1 (0.3 μM) in C_2H_5OH/H_2O (80:20) at pH 7.2 (0.01 M HEPES) upon the gradual addition of Hg^{2+} from 0.03 to 0.35 μM. Inset: the ratio intensity at 584 and 510 nm upon the gradual addition of Hg^{2+}.

The selectivity of BRP-1 for different metal ions was investigated. Various alkali, alkaline earth metal ions, and transition-metal ions (Na^+, Mg^{2+}, Ca^{2+}, Al^{3+}, Pb^{2+}, Cu^{2+}, Cd^{2+}, Fe^{3+}, Fe^{2+}, Zn^{2+}, Cr^{3+}, Co^{2+}, and Ni^{2+} etc.) were measured. Only the Ag^+ ion promoted a small fluorescence intensity enhancement at 584 nm and a distinct decrease at 510 nm, whereas the other metal ions did not induce any fluorescence or color changes of BRP-1 upon the addition of metal ions (10 equiv) (Figure S3 in the Supporting Information). The selectivity observed for Hg^{2+} over other metal ions was remarkably high. In addition, the ratiometric fluorescence changes resulting from the addition of Hg^{2+} was not influenced by the subsequent addition of other metal ions. Although the interference of Ag^+ was not negligible, the I_{584}/I_{510} ratio of BRP-1 showed good selectivity toward Hg^{2+} ions (Figure 3a). Due to a solvent mixture with 80% alcohol or acetonitrile content used in the experiment, the pH values obtained from the pH meter were different from that obtained in water. Therefore, the acid/base concentration was used to reveal the interaction between BRP-1-(BRP-2) and acid/base. The acid/base responses of BRP-1 and BRP-1 in the presence of Hg^{2+} (5.0 equiv) are shown in Figure 3b. These solutions remained stable over a wide concentration range of acid/base (from log[HCl] = −3.0 to log-[NaOH] = −5.0), suggesting that the response was insensitive to acid/base and the spirolactam form of BRP-1 was still preferred in that range in the absence of mercury ion.

Properties of sensor BRP-2: The mechanism of BRP-2 was different from BRP-1. In the presence of Hg^{2+}, the high thiophilicity of Hg^{2+} induced the ring opening of thiospirolactone in the rhodamine moiety; this was called a metal-coordination-induced ring-opening reaction. The ESI-MS spectra showed three kinds of binding ratio between Hg^{2+} and BRP-2, as shown in Figure 4. When Hg^{2+} (1.0 equiv) was added to BRP-2 in H_2O/CH_3CN, the signal at *m*/*z* 961.2106 given in Figure 4, corresponding to $[Hg(BRP\text{-}2)Cl]^+$ (labeled 2 in Figure 4) was clearly observed, which indicated a 1:1 binding ratio between Hg^{2+} and BRP-2 existed in solvent. The signal at *m*/*z* 825.2647 given in Figure 4, corresponding to $[Hg(BRP\text{-}2)_2]^{2+}$ (1:2) (labeled 1 in Figure 4) was also found in ESI-MS spectra. In the solvent, there was another complex (labeled 3 in Figure 4) at *m*/*z* 1685.9658 given in Figure 4, corresponded to $[Hg(BRP\text{-}2)_2Cl)]^+$. When the mercury salt was changed from chloride to perchloride, a single binding mode was obtained from ESI-MS measurements, as shown in Figure 4c. The signal at *m*/*z* 824.7800 corresponding to $[Hg(BRP\text{-}2)_2]^{2+}$ (1:2) was clearly observed. Due to the different coordinating ability of the counteran-

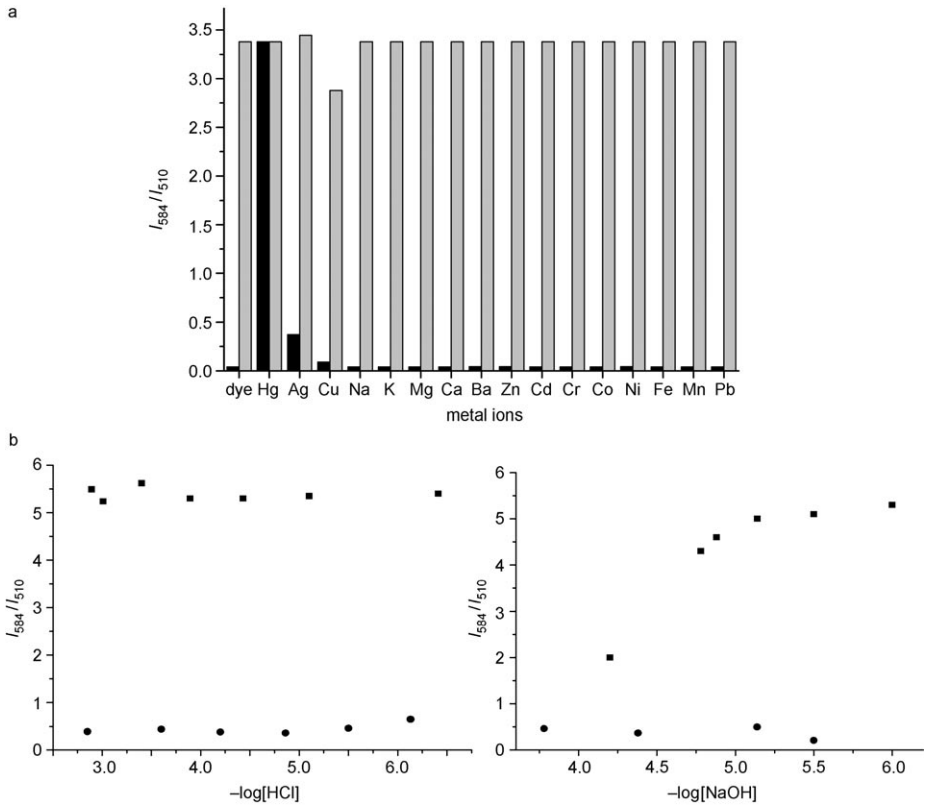

Figure 3. a) I_{584}/I_{510} ratio of BRP-1 (0.3 μM) in C_2H_5OH/H_2O (80:20 v/v, pH 7.2) in the presence of various metal ions (10 equiv). Black bars represent the addition of an excess of the appropriate metal ion (3 μM) to a 0.3 μM solution of BRP-1. Gray bars represent the subsequent addition of 3 μM Hg^{2+} to this solution. b) I_{584}/I_{510} ratio of BRP-1 (●) and BRP-1 in present of 5.0 equiv Hg^{2+} (■) in C_2H_5OH/H_2O (80:20 v/v) versus different concentrations of HCl and NaOH at room temperature ($\lambda_{ex}=488$ nm.)

ions, the binding complex between BRP-2 and Hg^{2+} would be different, which was also indicated in Job's plot (Figure S4 in the Supporting Information). Although Hg^{2+} with different counteranions could switch on the energy transfer of BRP-2 to similar degrees (Figure S5 in the Supporting Information), small but apparent differences in the extents of ratiometric changes in the two emissions were observed. Thus, in the application of BRP-2, the interference of counteranions is not negligible.

The Hg^{2+}-induced ring-opening reaction of thiospirolactone was similar to previously reported Hg^{2+}-induced ring-opening reactions.[38] The absorption and fluorescence titration of Hg^{2+} was also investigated by using 3.25 μM BRP-2 in acetonitrile/water (80/20 v/v). Upon the addition of Hg^{2+}, the trend of variation in absorption and emission spectra was similar to that of BRP-1. The changes of absorption and emission spectra are shown in Figure 5. The I_{584}/I_{510} ratio was linearly proportional to the Hg^{2+} concentration over the range of 6.5 to 62.5 μM (1.3–12.5 ppm). The response to Hg^{2+} of BRP-2 was also very fast and spectral data were recorded within 5 min after the addition of Hg^{2+}.

Changes in the I_{584}/I_{510} ratio of BRP-2 caused by other metal ions are shown in Figure 6a. BRP-2 showed an excellent selectivity toward Hg^{2+}. The other metal ions did not cause any apparent changes in the optical properties of BRP-2 upon the addition of metal ions (10 equiv) (Figure 6a). In addition, the enhancement in fluorescence intensity at 585 nm resulting from the addition of Hg^{2+} was not influenced by the subsequent addition of other metal ions. Thus, BRP-2 displayed better selectivity toward Hg^{2+} than BRP-1, the Hg^{2+} recognition of which was disrupted by Ag^{+}. BRP-2 also exhibited insensitivity to acid/base over a wide concentration range (Figure 6b). However, the Hg^{2+} detection limit of BRP-2 was only on the ppm scale, thus its sensitivity was much lower than that of BRP-1, the detection limit of which was on the ppb scale. This could be ascribed to their different recognition mechanisms. The irreversible ring-opening reaction of BRP-1 induced by Hg^{2+} might be much more efficient than the reversible reaction of BRP-2. Despite its lower sensitivity relative to BRP-1, BRP-2 also had advantages as a potential reusable sensor because its coordination with Hg^{2+} was reversible and it could be recovered from the complex of Hg^{2+}–BRP-2, if excess competing coordinating reagents, such as KI (Figure S4 in the Supporting Information), were added to attract Hg^{2+}.

Intracellular imaging for Hg^{2+} of BRP-1: To further confirm the applicability of these two sensors in biological imaging, fluorescence microscopy images in living cells were investigated. Generally, there are two methods used for the imaging of metal ions in living cells during cellular incubation of sensors and metal ions in literature.[47,48] One method is to incubate cells first with ions for a certain length of time and then to incubate the cells with fluorescent sensors. The second method involves the incubation of first the sensor and then the addition of ions. Some chemists, such as Tae and co-workers,[47] often used the former method in the cellular imaging of metal ions. This method is suitable for turn-on sensors and is usually encountered in analytical chemistry. The latter was often used by others in imaging experiments not only with turn-on sensors,[48,49] but also with ratiometric sensors.[50] In our experiments, we decided that the latter method would be more appropriate for ratiometric sensors. The process of visible fluorescence (from green to red) responses to metal ions could be demonstrated.

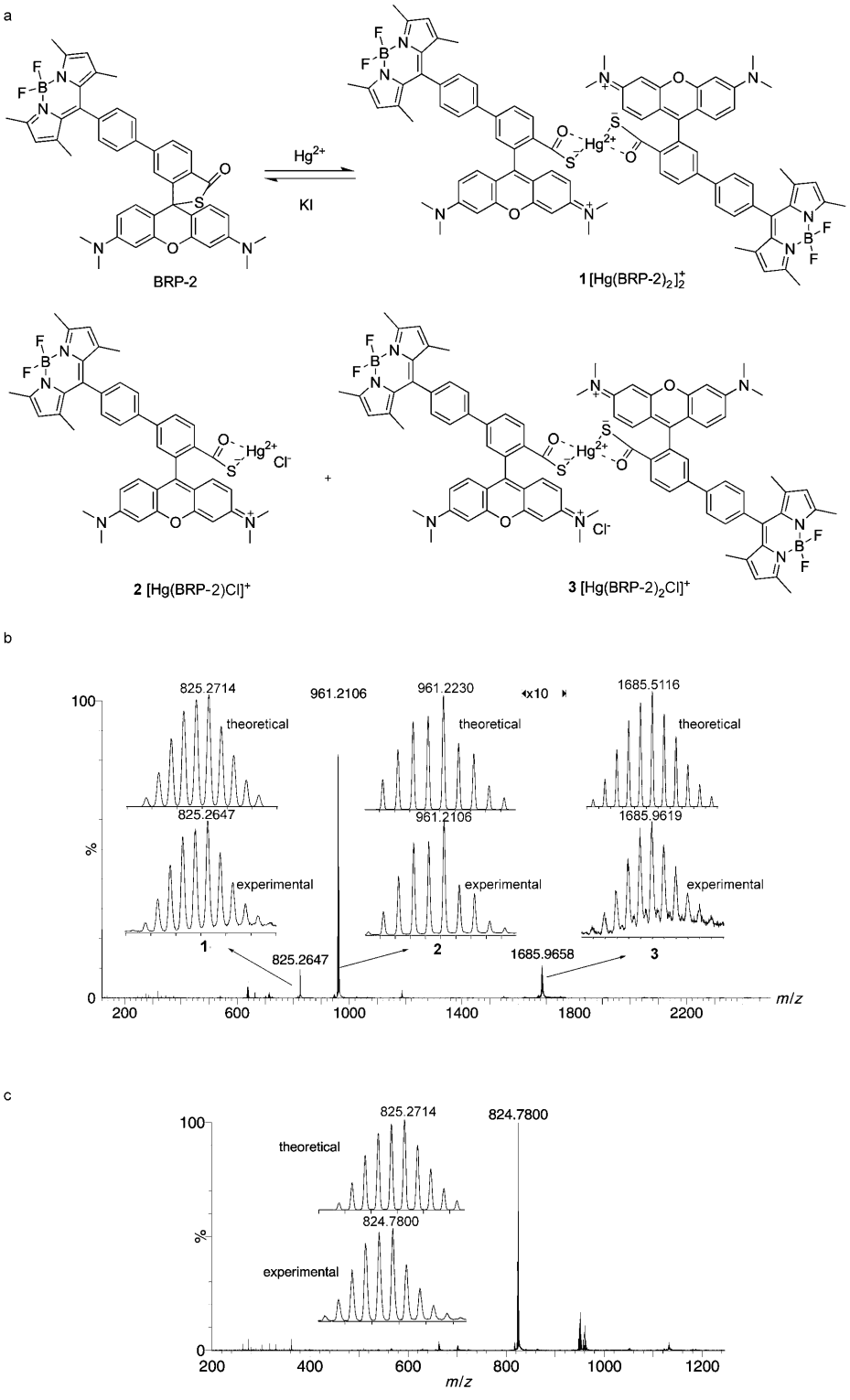

Figure 4. a) Hg^{2+}-coordination-induced ring-opening reaction of BRP-2. b) ESI-MS spectrum of BRP-2 in the presence of $HgCl_2$ (1 equiv) in H_2O/CH_3CN. c) ESI-MS of BRP-2 in the presence of $Hg(ClO_4)_2$ (1 equiv) in H_2O/CH_3CN solvent.

In preliminary experiments, an inverted fluorescence microscope was used to observe the process of Hg^{2+} entering into and diffusing within Hela cells. The cells were incubated with these sensors (2.5 μM) for 15 min at room temperature and then the cells were washed three times with phosphate-buffered saline (PBS; pH 7.4). Upon excitation with blue light, a strong green intracellular fluorescence was detected, which indicated that both sensors were cell permeable. Supplementing cells incubated with sensor BRP-1 with 2.5 μM $HgCl_2$ in PBS for 10 min at room temperature resulted in significant color changes, as shown in Figure 7a. The response of BRP-1 to Hg^{2+} was very fast. Hela cells showed color changes from green to yellow–orange after incubation with Hg^{2+} for 6 min. After 10 min, orange–red cell images were obtained. The above results demonstrated that BRP-1 could sense and image intracellular mercury ions sensitively and quickly. BRP-2 also exhibited good cell permeability and bright green intracellular fluorescence. However, the response of BRP-2 to intracellular Hg^{2+} was much slower and less sensitive than that of BRP-1. To clearly demonstrate the color changes, a high concentration of Hg^{2+} (10 equiv) was used in the cellular imaging of BRP-2. As shown in Figure 7b, supplementing Hela cells incubated with sensor BRP-2 with 25 μM $HgCl_2$ (10 equiv) in PBS at room temperature resulted in gradual color changes from green to green–yellow after 2 h. After Hela cells were incubated with mercury ions for 3 h, orange cell images were observed. Compared with BRP-1, even in the presence of Hg^{2+} (10 equiv), a longer equilibrium time of BRP-2 to Hg^{2+} was required to achieve apparent fluorescent color changes. Although BRP-2 responded to Hg^{2+} in aqueous solution as quickly as BRP-1 did, its lower performance in living cells might be ascribed to the recognition mechanism on coordination-induced reaction. There

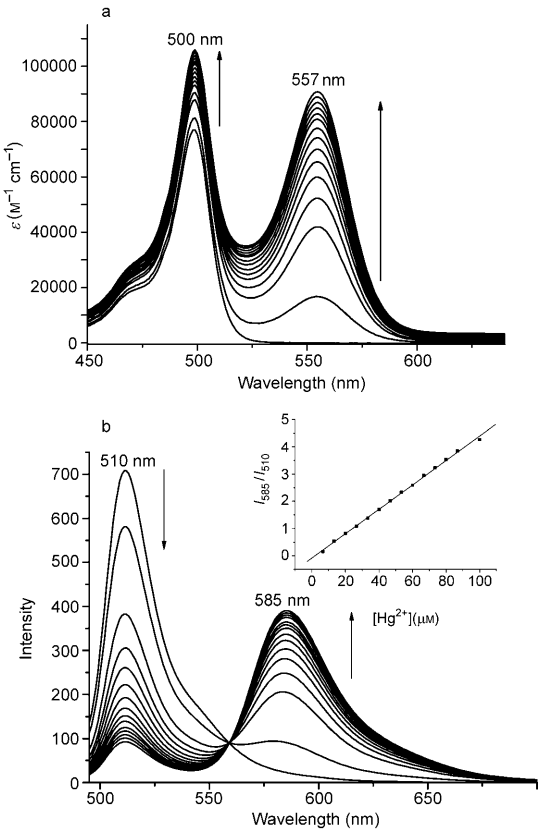

Figure 5. Changes in the absorption (a) and emission spectra (b) of BRP-2 (3.25 μM) in CH_3CN/H_2O (80:20) at pH 7.2 (0.01 M HEPES) upon the gradual addition of Hg^{2+} from 6.5 to 62.5 μM. Inset: the ratio intensity at 585 and 510 nm upon the gradual addition of Hg^{2+}.

are many thiol-containing biological molecules that might compete with BRP-2 in the coordination of mercury ions.

Quantitatively detecting intracellular mercury ions required ratiometric imaging data that could not be obtained by an ordinary inverted fluorescence microscope. Thus, confocal microscopy experiments were further carried out. Different from an inverted fluorescence microscope, a confocal microscope has multichannel detectors, which provide good opportunities to observe the changes of emission intensity at different wavelengths. During the confocal imaging experiments, an Ar laser provided the single excitation wavelength (488 nm) that was suitable for the absorption of the BODIPY fluorophore. Then, in this experiment fluorescence images were obtained at (515±15) (green channel) and (590±25) nm (red channel), respectively. Ratiometric sensor BRP-1 was chosen as an indicator due to its fast response to mercury ions. MCF-7 cells incubated with BRP-1 (2.5 μM) for 15 min at room temperature showed a clear green intracellular fluorescence, as shown in Figure 8a. In the green channel a strong green fluorescence could be seen. Meanwhile, there was little red fluorescence in the red channel, which indicated that BRP-1 mainly existed in the form of the spirolactam. As shown in the ratio imaging in Figure 8a, there were no significant ratio changes of $I_{590\pm25}/I_{515\pm15}$. When cells stained with BRP-1 were incubated with $HgCl_2$ (2.5 μM) for 5 min, the color of the MCF-7 cells showed significant changes from green to yellow–orange. In the imaging, partial quenching of the green fluorescence intensity and a partial increase in the red fluorescence intensity was observed (Figure 8b). Because Hg^{2+} only partially reacted to BRP-1 within 5 min, the pseudo-color of the ratio imaging in Figure 8b showed real-time responses between Hg^{2+} and BRP-1 in different cells. When MCF-7 cells stained with BRP-1 were incubated with $HgCl_2$ for 10 min, the green fluorescence intensity decreased significantly and the red fluorescence intensity remarkably increased (Figure 8c). The pseudo-color of ratio imaging in Figure 8c showed different distributions of Hg^{2+} in MCF-7 cell. By producing ratio images, it is possible to construct a map showing local ion concentrations throughout the field of view.

The fast and drastic green-to-red color changes of BRP-1 in intracellular Hg^{2+} imaging could be clearly distinguished by using confocal fluorescence microscopy; this satisfied the requirement for real-time observations. The visible color changes should indicate to the two narrow emission bands of BODIPY and TMR fluorophores. These two well-separated emissions of BRP-1 by a single excitation wavelength (488 nm) were highly desirable for fluorescence ratiometric sensing, which not only ensured the detection accuracy, as discussed in the Introduction, but also simplified the excitation source to a single one and reduced the expense of the detection device. The ratio changes of fluorescence intensities at 584 and 510 nm were converted into a pseudo-color, which could show the distribution of Hg^{2+} in a cell.

Conclusion

An intramolecular BRP FRET cassette with BODIPY and TMR fluorophores was constructed based on a spectral overlap-modulated FRET strategy. A rigid biphenyl group, which favored through-bond energy transfer and kept a fixed donor–acceptor distance and orientation, was used to connect donor and acceptor moieties. To realize such a connection, regioisomerically pure 5′-Br-TMR, a useful synthetic building block, was developed according to a stepwise synthetic strategy. The BODIPY moiety was connected to 5′ position of TMR efficiently through Suzuki coupling. BRP was the first FRET platform in which the 2′-carboxyl group of the rhodamine unit was preserved for further modifications. The spectral changes in different solvents indicated that the FRET of BRP could be switched off and on under proper conditions and the energy-transfer efficiency was up to 99% in the on state. As a versatile FRET platform, chemical modifications on BRP were convenient and straightforward. Two Hg^{2+} sensors, BRP-1 and BRP-2, were efficiently developed on the BRP platform as representative ratiometric sensors. The recognition mechanisms of BRP-1 and BRP-2 were different: the mechanism for BRP-1 was an irreversible ring-opening reaction induced by mercury

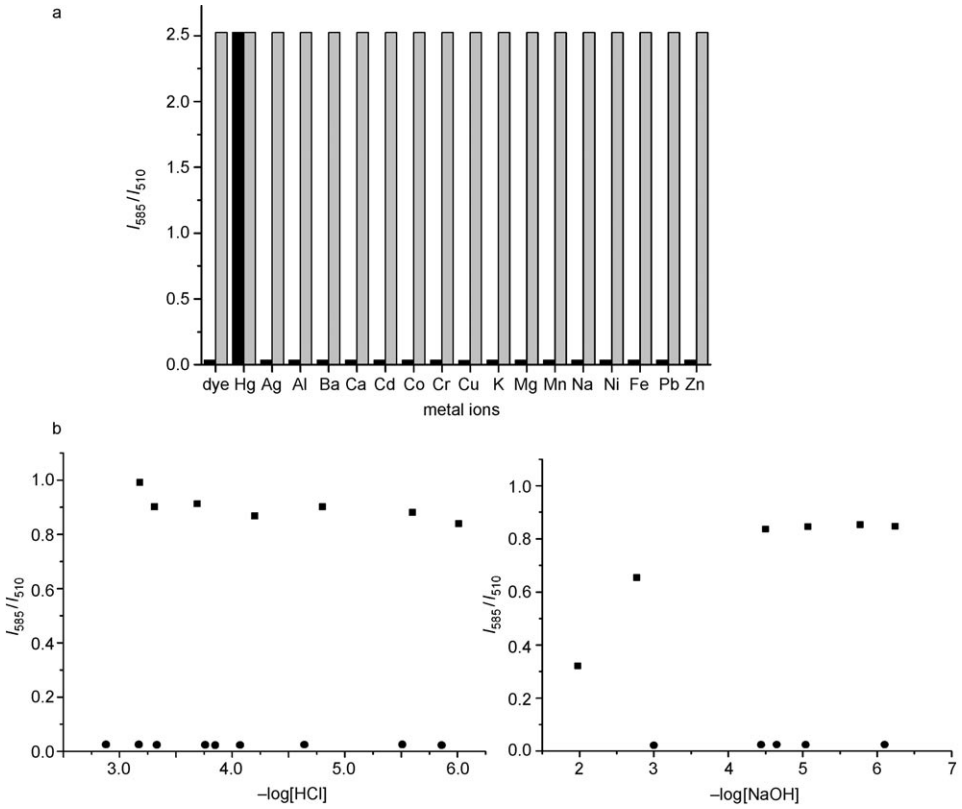

Figure 6. a) I_{584}/I_{510} ratios of BRP-2 (3.25 μM) in CH_3CN/H_2O (80:20 v/v, pH 7.2) in the presence of various metal ions (10 equiv). Black bars represent the addition of an excess of the appropriate metal ion (32.5 μM) to a 3.25 μM solution of BRP-2. Gray bars represent the subsequent addition of 32.5 μM Hg^{2+} to this solution. b) I_{585}/I_{510} ratio of BRP-2 (●) and BRP-2 in presence of Hg^{2+} (5 equiv; ■) in CH_3CN/H_2O (80:20 v/v) versus different concentrations of HCl and NaOH at room temperature ($\lambda_{ex}=488$ nm.)

ions, but the ring-opening reaction of BRP-2 was reversible. Excited at the single excitation wavelength (488 nm), both sensors exhibited clear Hg^{2+}-induced changes in the intensity ratio of the two strong emission bands of BODIPY and rhodamine. While both were applicable to the imaging of Hg^{2+} in living cells, BRP-1 displayed higher sensitivity and a faster response. There have already been many turn-on rhodamine spirocyclic sensors, the numbers of which are still increasing rapidly. All experiences in turn-on rhodamine spirocyclic sensors may be used in ratiometric sensors based on a FRET switch-on strategy. The BRP platform, as well as its analogues, should be applicable to a broad range of ratiometric sensors for various analytes.

Experimental Section

General: All chemicals were obtained from commercial suppliers and used without further purification. The silica gel used was 200–300 mesh. ^1H and ^{13}C NMR spectra were measured on Varian 400 and Bruker 400 spectrometers in $CDCl_3$ or $[D_6]DMSO$ with tetramethylsilane (TMS) as the internal reference. Mass spectra were measured on a UPLC/Q-TOF mass spec-

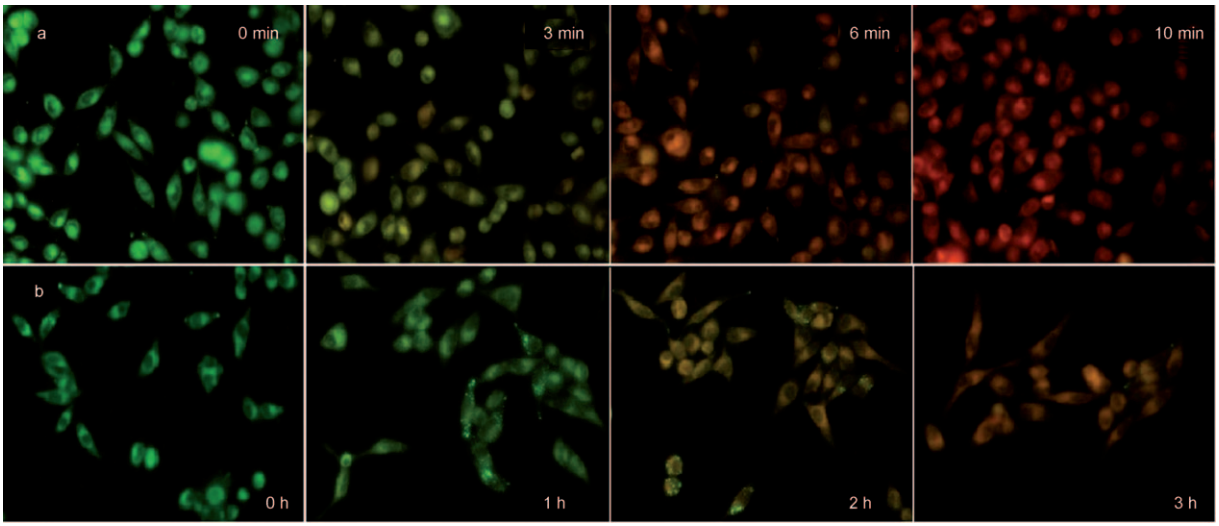

Figure 7. Images of Hela cells under an inverted fluorescent microscope. a) The cells were incubated with BRP-1 (2.5 μM) for 15 min at room temperature. Fluorescence images of Hela cells then further incubated with $HgCl_2$ (2.5 μM) for 10 min were recorded. b) The cells were incubated with BRP-2 (2.5 μM) for 15 min at room temperature. Fluorescence image of Hela cells incubated with 25 μM $HgCl_2$ for 3 h at room temperature were recorded.

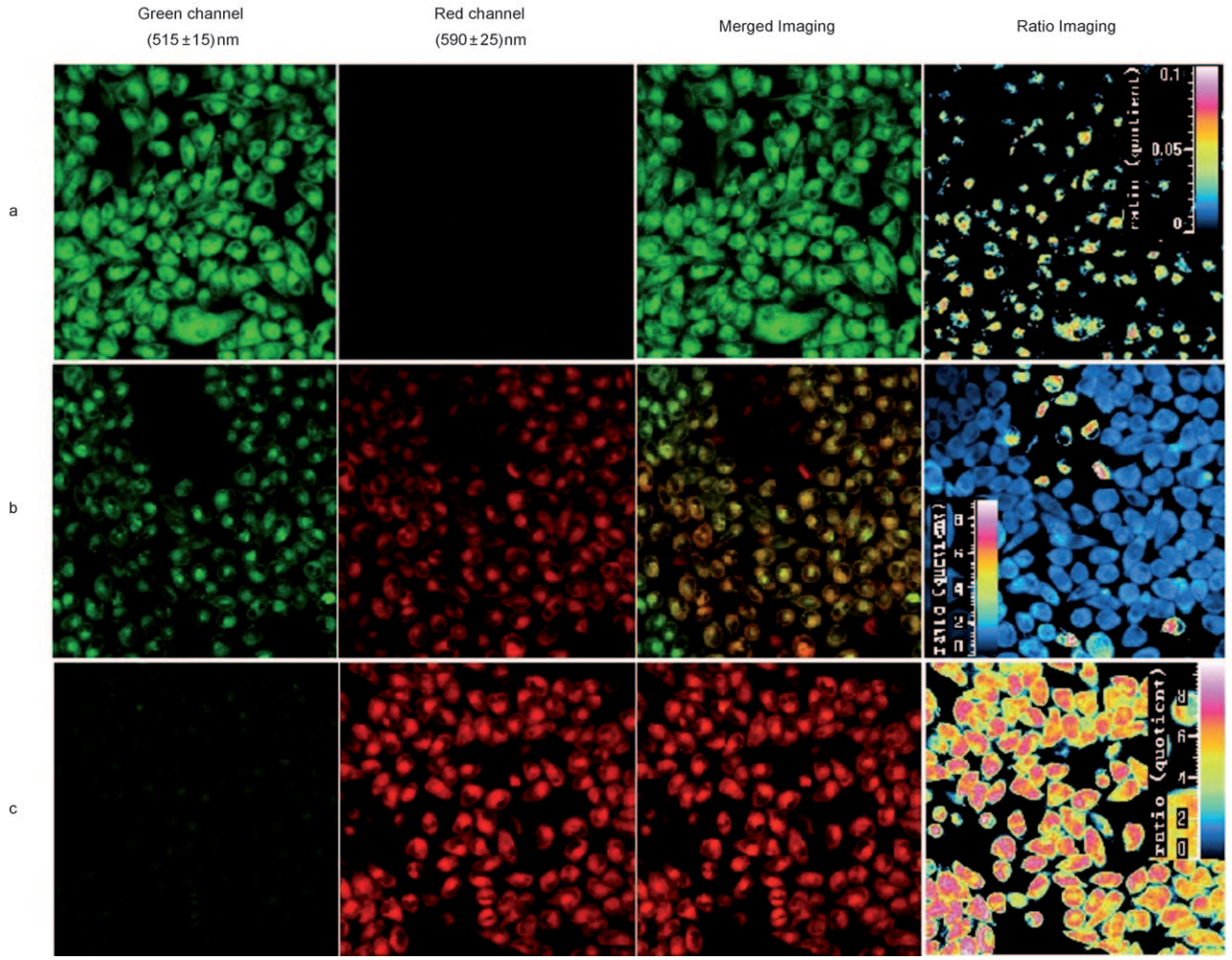

Figure 8. Confocal fluorescence imaging of Hg^{2+} in MCF-7 cell with BRP-1 (2.5 μM) for 15 min. a) cells without Hg^{2+}. b) cells incubated with $HgCl_2$ (2.5 μM) for 5 min. c) cells incubated with $HgCl_2$ (2.5 μM) for 10 min.

trometer. Fluorescence spectra were measured on spectroflurophotometer FP-6500. Absorption spectra were determined on a UV/Vis spectrophotometer HP-8453.

Platform BRP: A mixture of compound **1** (600 mg, 1.33 mmol), 5′-bromotetramethylrhodamine (500 mg, 0.98 mmol), PPh_3 (46 mg, 0.18 mmol), $Pd(OAC)_2$ (6.6 mg, 0.03 mmol), Na_2CO_3 (415.5 mg, 3.92 mmol), and *n*-propanol/methanol (20 mL/20 mL) were placed in a 100 mL round-bottomed flask with a magnetic stirrer bar under a nitrogen atmosphere . The mixture was heated at 75 °C for 6 h. Then the crude product was purified by silica-gel column chromatography with a mixture of CH_2Cl_2/CH_3OH/$N(C_2H_5)_3$ (100:3.5:2.5, v/v) as the eluent. A red solid was obtained. This solid was dissolved in methanol (5 mL) and added to HBF_4 (2 M), then the precipitate was collected and recrystalized in mixture of dichloromethane and *n*-hexane. BRP was obtained as a bright black crystal (42 mg, 78 %). M.p. 274–276 °C; ^{1}H NMR (400 MHz, [D$_6$]DMSO, 25 °C, TMS): δ = 8.28 (d, ^3J(H,H) = 8.0 Hz, 1 H; Ar*H*), 8.23 (d, ^3J(H,H) = 7.2 Hz, 1 H; Ar*H*), 8.01 (d, ^3J(H,H) = 6 Hz, 2 H; Ar*H*), 7.89 (s,1 H; Ar*H*), 7.50 (d, ^3J(H,H) = 7.2 Hz, 2 H; Ar*H*), 7.06–6.89 (t, 6 H; Ar*H*), 6.18 (s, 2 H; pyrrole-C*H*), 3.21 (s, 12 H; $N(CH_3)_2$), 2.45 (s, 6 H; pyrrole-CH_3), 1.39 ppm (s, 6 H; pyrrole-CH_3); ^{13}C NMR (100 MHz, [D$_6$]DMSO, 25 °C, TMS): δ = 166.1, 156.5, 155.0, 142.6, 141.2, 138.2, 134.5, 131.3, 130.8, 130.5, 129.7, 128.8, 128.2, 127.8, 121.4, 114.3, 112.7, 96.2, 39.9, 14.2 ppm; HRMS (ES): *m*/*z* calcd for $C_{43}H_{40}BN_4O_3F_2$: 709.3162 [M^+]; found: 709.3134.

Sensor BRP-1: Hydrazine monohydrate (0.10 mL (excess)) was added to BRP (100 mg, 0.14 mmol) in MeOH (15 mL). The reaction solution was heated at 60 °C for 6 h. During the reaction the color of the solution changed from red to pink. Then, the solvent was removed in vacuo to give a red solid. This red solid was dissolved in DMF (15 mL) and then a solution of phenyl isothiocyanate (50 μL, 0.28 mmol) in DMF (1.5 mL) was added. The reaction mixture was heated at 60 °C for 4 h. The crude product was purified by silica-gel column chromatography with a mixture of CH_2Cl_2/CH_3OH (300:1, v/v) as the eluent. After recrystalization in mixture of dichloromethane and *n*-hexane, BRP-1 was obtained as red crystals (75 mg, 63 %). M.p. 242–245 °C; ^{1}H NMR (400 MHz, $CDCl_3$, 25 °C, TMS): δ = 8.13 (d, ^3J(H,H) = 8 Hz, 1 H; Ar*H*), 7.90 (dd, ^3J(H,H) = 8, ^4J(H,H) = 3.6 Hz, 1 H; Ar*H*), 7.70 (d, ^3J(H,H) = 8.4 Hz, 2 H; Ar*H*), 7.56 (s, 1 H; Ar*H*), 7.51(s, 1 H; Ar*H*), 7.33 (d, ^3J(H,H) = 8 Hz, 2 H; Ar*H*), 7.23–7.19 (t, ^3J(H,H) = 8 Hz, 2 H; Ar*H*), 7.14–7.10 (t, ^3J(H,H) = 8 Hz, 2 H; Ar*H*), 7.07(d, ^3J(H,H) = 8 Hz, 1 H; Ar*H*), 6.91(d, ^3J(H,H) = 3.6 Hz, 1 H; Ar*H*), 6.61 (d, ^3J(H,H) = 8.8 Hz, 1 H; Ar*H*), 6.52 (d, ^3J(H,H) = 2.8 Hz, 2 H; Ar*H*), 6.37 (dd, ^3J(H,H) = 8.8, ^4J(H,H) = 2.4 Hz, 2 H; Ar*H*), 5.97 (s, 2 H; pyrrole-C*H*), 2.97 (s, 12 H; $N(CH_3)_2$), 2.55 (s, 6 H; pyrrole-CH_3), 1.38 ppm (s, 6 H; pyrrole-CH_3); ^{13}C NMR (100 MHz, $CDCl_3$, 25 °C, TMS): δ = 182.8, 166.9, 155.9, 154.2, 152.2, 151.2, 146.5, 143.1, 140.9, 140.4, 137.9, 135.5, 131.5, 129.1, 128.7, 128.5, 128.4, 127.7, 126.2, 125.1, 124.7, 123.1, 121.5, 109.4, 105.2, 99.7, 67.5, 40.3, 14.8 ppm; HRMS (ES): *m*/*z* calcd for $C_{50}H_{47}BN_7O_2F_2S$: 858.3573 [M^+]; found: 858.3544.

Sensor BRP-2: A solution of BRP (100 mg, 0.14 mmol) in dry 1,2-dichloroethane (20 mL) was stirred until the solid dissolved completely, and phosphorus oxychloride (18 μL) was added with vigorous stirring at

room temperature for 5 min. Then, the solution was heated at reflux for 2 h. The reaction mixture was cooled and evaporated in vacuo to give BRP acid chloride. The crude acid chloride was dissolved in acetonitrile (15 mL) and added dropwise to a solution of Na_2S (22 mg, 0.28 mmol) in water (5 mL). After stirring overnight, the crude product was purified by silica-gel column chromatography with a mixture of dichloromethane and *n*-hexane (1.5:1, v/v) as the eluent. BRP-2 was obtained as red crystals (74 mg, 73%) M.p. 278–281 °C; ^{1}H NMR (400 MHz, $CDCl_3$, 25 °C, TMS): δ = 7.95 (d, ^3J(H,H) = 8.0 Hz, 1H; Ar*H*), 7.78 (d, ^3J(H,H) = 8.0 Hz, 1H; Ar*H*), 7.62 (d, ^3J(H,H) = 8.0 Hz, 2H; Ar*H*), 7.46 (s, 1H; Ar*H*) 7.29 (d, ^3J(H,H) = 8.0 Hz, 2H; Ar*H*), 6.84 (d, ^3J(H,H) = 8.0 Hz, 2H; Ar*H*), 6.40 (d, ^3J(H,H) = 8.0 Hz, 4H; Ar*H*), 5.96 (s, 2H; pyrrole-C*H*), 2.97 (s, 12H; N-(CH_3)$_2$), 2.54 (s, 6H; pyrrole-CH_3), 1.37 ppm (s, 6H; pyrrole-CH_3); ^{13}C NMR (100 MHz, $CDCl_3$, 25 °C, TMS): δ = 196.9, 158.7, 155.9, 152.2, 151.3, 146.3, 143.2, 141.1, 140.1, 135.4, 131.4, 129.9, 128.8, 128.3, 127.8, 125.4, 123.4, 121.5, 109.7, 109.2, 98.8, 62.7, 40.4, 14.9, 14.7 ppm; HRMS (ES): *m*/*z* calcd for $C_{43}H_{40}BN_4O_2F_2S$: 725.2933 [M^+]; found: 725.2906.

Acknowledgements

We thank the NSF of China (no. 20876022), the Fundamental Research Funds for the Central University (DUT10ZD114) and the Program for Changjiang Scholars and Innovative Research Team in University (IRT0711) for financial support. We also thank Dr. Liji Jin (Dalian University of Technology) for help with cell culture experiments and Dr. Xiaolin Yuan (Dalian University) for help with confocal microscopy experiments.

[1] V. Amendola, L. Fabbrizzi, M. Licchelli, C. Mangano, P. Pallavicini, L. Parodi, A. Poggi, *Coord. Chem. Rev.* **1999**, *190–192*, 649–669.
[2] L. Prodi, F. Bolletta, M. Montalti, N. Zaccheroni, *Coord. Chem. Rev.* **2000**, *205*, 59–83.
[3] a) A. P. de Silva, H. Q. N. Gunaratne, T. Gunnlaugsson, A. J. M. Huxley, C. P. McCoy, J. T. Rademacher, T. E. Rice, *Chem. Rev.* **1997**, *97*, 1515–1566; b) F. L. Song, S. Watanabe, P. E. Floreancig, K. Koide, *J. Am. Chem. Soc.* **2008**, *130*, 16460–16461; c) K. Komatsu, K. Kikuchi, H. Kojima, Y. Urano, T. Nagano, *J. Am. Chem. Soc.* **2005**, *127*, 10197–10204; d) S. Fakih, M. Podinovskaia, X. Kong, H. L. Collins, U. E. Schaible, R. C. Hider, *J. Med. Chem.* **2008**, *51*, 4539–4552; e) E. M. Nolan, S. J. Lippard, *J. Am. Chem. Soc.* **2003**, *125*, 14270–14271; f) D. W. Domaille, L. Zeng, C. J. Chang, *J. Am. Chem. Soc.* **2010**, *132*, 1194–1195; g) Q. W. He, E. W. Miller, A. P. Wong, C. J. Chang, *J. Am. Chem. Soc.* **2006**, *128*, 9316–9317.
[4] R. Y. Tsien in *Fluorescent Chemosensors for Ion and Molecule Recognition* (Ed.: A. W. Czarnik), ACS, Washington, DC, **1993**, pp. 130–146.
[5] a) K. Kavallieratos, J. M. Rosenberg, W. Z. Chen, T. Ren, *J. Am. Chem. Soc.* **2005**, *127*, 6514–6515; b) S. K. Kim, S. H. Lee, J. Y. Lee, J. Y. Lee, R. A. Bartsch, J. S. Kim, *J. Am. Chem. Soc.* **2004**, *126*, 16499–16506; c) M. H. Ha-Thi, M. Penhoat, V. Michelet, I. Leray, *Org. Lett.* **2007**, *9*, 1133–1136; d) S. Y. Moon, N. J. Youn, S. M. Park, S. K. Chang, *J. Org. Chem.* **2005**, *70*, 2394–2397.
[6] K. Rurack, U. Resch-Genger, *Chem. Soc. Rev.* **2002**, *31*, 116–127.
[7] a) J. L. Bricks, A. Kovalchuk, C. Trieflinger, M. Nofz, M. Buschel, A. I. Tolmachev, J. Daub, K. Rurack, *J. Am. Chem. Soc.* **2005**, *127*, 13522–13529; b) Y. J. Jang, E. J. Jun, Y. J. Lee, Y. S. Kim, J. S. Kim, J. Yoon, *J. Org. Chem.* **2005**, *70*, 9603–9606; c) B. A. Wong, S. Friedle, S. J. Lippard, *J. Am. Chem. Soc.* **2009**, *131*, 7142–7152; d) A. L. Garner, F. L. Song, K. Koide, *J. Am. Chem. Soc.* **2009**, *131*, 5163–5171; e) S. C. Dodani, Q. W. He, C. J. Chang, *J. Am. Chem. Soc.* **2009**, *131*, 18020–180201; f) X. J. Peng, J. J. Du, J. L. Fan, J. Y. Wang, Y. K. Wu, J. Z. Zhao, S. G. Sun, T. Xu, *J. Am. Chem. Soc.* **2007**, *129*, 1500–1502; g) J. H. Do, H. N. Kim, J. Yoon, J. S. Kim, H. J. Kim, *Org. Lett.* **2010**, *12*, 932–934;h) R. D. Carpenter, A. S. Verkman, *Org. Lett.* **2010**, *12*, 1160–1163; i) S. V. Wegner, A. Okesli, P. Chen, C. He, *J. Am. Chem. Soc.* **2007**, *129*, 3474–3475.
[8] a) J. V. Ros-Lis, B. García, D. Jiménez, R. Martínez-Máñez, F. Sancenón, J. Soto, F. Gonzalv, M. C. Valldecabres, *J. Am. Chem. Soc.* **2004**, *126*, 4064–4065; b) M. Santra, D. Ryu, A. Chatterjee, S. K. Ko, I. Shin, K. H. Ahn, *Chem. Commun.* **2009**, 2115–2117;c) J. J. Gassensmith, J. M. Baumes, B. D. Smith, *Chem. Commun.* **2009**, 6329–6338.
[9] a) H. N. Kim, M. H. Lee, H. J. Kim, J. S. Kim, J. Yoon, *Chem. Soc. Rev.* **2008**, *37*, 1465–1472; b) M. Beija, C. A. M. Afonso, J. M. G. Martinho, *Chem. Soc. Rev.* **2009**, *38*, 2410–2433; c) X. Zhang, Y. Shiraishi, T. Hirai, *Tetrahedron Lett.* **2007**, *48*, 5455–5459; d) W. S. Zhang, B. Tang, X. Liu, Y. Y. Liu, K. H. Xu, J. P. Ma, L. L. Tong, G. W. Yang, *Analyst* **2009**, *134*, 367–371.
[10] a) Y. Zhao, X. B. Zhang, Z. X. Han, L. Qiao, C. Y. Li, L. X. Jian, G. L. Shen, R. Q. Yu, *Anal. Chem.* **2009**, *81*, 7022–7030; b) V. Dujols, F. Ford, A. W. Czarnik, *J. Am. Chem. Soc.* **1997**, *119*, 7386–7387; c) Y. Zhou, F. Wang, Y. Kim, S. J. Kim, J. Yoon, *Org. Lett.* **2009**, *11*, 4442–4445; d) X. Zhang, Y. Shiraishi, T. Hirai, *Org. Lett.* **2007**, *9*, 5039–5042.
[11] a) J. H. Soh, K. M. K. Swamy, S. K. Kim, S. Kim, S. H. Lee, J. Yoon, *Tetrahedron Lett.* **2007**, *48*, 5966–5969; b) W. Huang, P. Zhou, W. B. Yan, C. He, L. Q. Xiong, F. Y. Li, C. Y. Duan, *J. Environ. Monit.* **2009**, *11*, 330–335; c) Y. Shiraishi, S. Sumiya, Y. Kohno, T. Hirai, *J. Org. Chem.* **2008**, *73*, 8571–8574; d) H. Yang, Z. G. Zhou, K. W. Huang, M. X. Yu, F. Y. Li, T. Yi, C. H. Huang, *Org. Lett.* **2007**, *9*, 4729–4732; e) D. Y. Wu, W. Huang, C. Y. Duan, Z. H. Lin, Q. J. Meng, *Inorg. Chem.* **2007**, *46*, 1538–1540; f) J. H. Huang, Y. F. Xu, X. H. Qian, *J. Org. Chem.* **2009**, *74*, 2167–2170.
[12] a) S. Bae, J. Tae, *Tetrahedron Lett.* **2007**, *48*, 5389–5392; b) J. Mao, Q. He, W. S. Liu, *Talanta* **2010**, *80*, 2093–2098; c) L. Dong, C. Wu, X. Zeng, L. Mu, S. F. Xue, Z. Tao, J. X. Zhang, *Sensor Actuat. B-Chem.* **2010**, *145*, 433–437.
[13] a) J. Mao, Q. He, W. S. Liu, *Anal. Bioanal. Chem.* **2010**, *396*, 1197–1203; b) J. Mao, L. Wang, W. Dou, X. L. Tang, Y. Yan, W. S. Liu, *Org. Lett.* **2007**, *9*, 4567–4570; c) A. J. Weerasinghe, C. Schmiesing, E. Sinn, *Tetrahedron Lett.* **2009**, *50*, 6407–6410.
[14] a) O. A. Egorova, H. Seo, A. Chatterjee, K. H. Ahn, *Org. Lett.* **2010**, *12*, 401–403; b) Y. K. Yang, S. Lee, J. Tae, *Org. Lett.* **2009**, *11*, 5610–5613; c) M. J. Jou, X. Chen, K. M. K. Swamy, H. N. Kim, H. J. Kim, S. G. Lee, J. Yoon, *Chem. Commun.* **2009**, 7218–7220.
[15] J. Y. Kwon, Y. J. Jang, Y. J. Lee, K. M. Kim, M. S. Seo, W. Nam, J. Yoon, *J. Am. Chem. Soc.* **2005**, *127*, 10107–10111.
[16] A. Chatterjee, M. Santra, N. Won, S. Kim, J. K. Kim, S. B. Ki, K. H. Ahn, *J. Am. Chem. Soc.* **2009**, *131*, 2040–2041.
[17] a) S. Kenmoku, Y. Urano, H. Kojima, T. Nagano, *J. Am. Chem. Soc.* **2007**, *129*, 7313–7318; b) X. Q. Chen, X. C. Wang, S. J. Wang, W. Shi, K. Wang, H. M. Ma, *Chem. Eur. J.* **2008**, *14*, 4719–4724; c) H. Zheng, G. O. Shang, S. Y. Yang, X. Gao, J. G. Xu, *Org. Lett.* **2008**, *10*, 2357–2360; d) H. Kojima, M. Hirotani, Y. Urano, K. Kikuchi, T. Higuchi, T. Nagano, *Tetrahedron Lett.* **2000**, *41*, 69–72.
[18] a) H. L. Li, J. L. Fan, J. Y. Wang, M. Z. Tian, J. J. Du, S. G. Sun, P. P. Sun, X. J. Peng, *Chem. Commun.* **2009**, 5904–5906; b) M. M. Pires, J. Chmielewski, *Org. Lett.* **2008**, *10*, 837–840; c) B. Tang, Y. L. Xing, P. Li, N. Zhang, F. B. Yu, G. W. Yang, *J. Am. Chem. Soc.* **2007**, *129*, 11666–11667.
[19] a) H. Lam, Y. Kostov, G. Rao, L. Tolosa, *Rev. Sci. Instrum.* **2009**, *80*, 124302–1–124302–7; b) G. Laczko, I. Gryczynski, Z. Gryczynski, W. Wiczk, H. Malak, J. R. Lakowicz, *Rev. Sci. Instrum.* **1990**, *61*, 2331–2337.
[20] a) T. Komatsu, Y. Urano, Y. Fujikawa, T. Kobayashi, H. Kojima, T. Terai, K. Hanaoka, T. Nagano, *Chem. Commun.* **2009**, 7015–7017; b) Z. Xu, J. Yoon, D. R. Spring, *Chem. Commun.* **2010**, *46*, 2563–2565; c) J. B. Wang; Y. Xiao; Z. C. Zhang, X. H. Qian, *J. Mater. Chem.* **2005**, *15*, 2836–2839; Y. Xiao; Z. C. Zhang, X. H. Qian, *J. Mater. Chem.* **2005**, *15*, 2836–2839.
[21] a) C. Hippius, F. Schlosser, M. O. Vysotsky, V. BDhmer, F. J. Wurthner, *J. Am. Chem. Soc.* **2006**, *128*, 3870–3871; b) G. Cicchetti, M. Biernacki, J. Farquharson, P. G. Allen, *Biochemistry* **2004**, *43*, 1939–1949; c) A. Ono, H. Togashi, *Angew. Chem.* **2004**, *116*, 4400–4402; *Angew. Chem. Int. Ed.* **2004**, *43*, 4300–4302; d) A. Coskun, E. U.

Akkaya, *J. Am. Chem. Soc.* **2005**, *127*, 10464–10465; e) R. Guliyev, A. Coskun, E. U. Akkaya, *J. Am. Chem. Soc.* **2009**, *131*, 9007–9013.
[22] X. L. Zhang, Y. Xiao, X. H. Qian, *Angew. Chem.* **2008**, *120*, 8145–8149; *Angew. Chem. Int. Ed.* **2008**, *47*, 8025–8029.
[23] M. H. Lee, H. J. Kim, S. Yoon, N. Park, J. S. Kim, *Org. Lett.* **2008**, *10*, 213–216.
[24] G. Q. Shang, X. Gao, M. X. Chen, H. Zheng, J. G. Xu, *J. Fluoresc.* **2008**, *18*, 1187–1192.
[25] Z. G. Zhou, M. X. Yu, H. Yang, K. W. Huang, F. Y. Li, T. Yi, C. H. Huang, *Chem. Commun.* **2008**, 3387–3389.
[26] M. Suresh, S. Mishra, S. K. Mishra, E. Suresh, A. K. Mandal, A. Shrivastav, A. Das, *Org. Lett.* **2009**, *11*, 2740–2743.
[27] a) L. M. S. Loura, A. Fedorov, M. Prieto, *J. Phys. Chem. B* **2000**, *104*, 6920; b) L. M. S. Loura, M. Prieto, *J. Phys. Chem. B* **2000**, *104*, 6911; c) B. Valeur, *Molecular Fluorescence: Principles and Applications*, Wiley-VCH, Weinheim, **2001**.
[28] a) H. Langhals, S. Saulich, *Chem. Eur. J.* **2002**, *8*, 5630–5643; b) R. Ziessel, C. Goze, G. Ulrich, *Chem. Eur. J.* **2005**, *11*, 7366–7378.
[29] A. Harriman, L. Mallon, R. Ziessel, *Chem. Eur. J.* **2008**, *14*, 11461–11473.
[30] a) K. E. Sapsford, L. Berti, I. L. Medintz, *Angew. Chem.* **2006**, *118*, 4676–4704; *Angew. Chem. Int. Ed.* **2006**, *45*, 4562–4588; b) Z. F. Walls, S. S. Gambhir, *Bioconjugate Chem.* **2008**, *19*, 178–184; c) E. G. Matveeva, Z. Gryczynski, D. R. Stewart, I. Gryczynski, *J. Lumin.* **2009**, *129*, 1281–1285; d) Z. S. Wu, H. Zhou, S. B. Zhang, X. B. Zhang, G. L. Shen, R. Q. Yu, *Chem. Commun.* **2010**, *46*, 2232–2234; e) T. Komatsu, K. Kikuchi, H. Takakusa, K. Hanaoka, T. Ueno, M. Kamiya, Y. Urano, T. Nagano, *J. Am. Chem. Soc.* **2006**, *128*, 15946–15947; f) W. Y. Lin, L. Yuan, Z. M. Cao, Y. M. Feng, J. Z. Song, *Angew. Chem.* **2010**, *122*, 385–389; *Angew. Chem. Int. Ed.* **2010**, *49*, 375–379.
[31] a) J. Y. Han, O. Gonzalez, A. Aguilar-Aguilar, E. Pena-Cabrera, K. Burgess, *Org. Biomol. Chem.* **2009**, *7*, 34–36; b) R. Bandichhor, A. D. Petrescu, A. Vespa, A. B. Kier, F. Schroeder, K. Burgess, *J. Am. Chem. Soc.* **2006**, *128*, 10688–10689.
[32] T. G. Kim, J. C. Castro, A. Loudet, J. G. S. Jiao, R. M. Hochstrasser, K. Burgess, M. R. Topp, *J. Phys. Chem. A* **2006**, *110*, 20–27.
[33] a) J. Y. Liu, H. S. Yeung, W. Xu, X. Y. Li, D. K. P. Ng, *Org. Lett.* **2008**, *10*, 5421–5424; b) G. Ulrich, R. Ziessel, A. Harriman, *Angew. Chem.* **2008**, *120*, 1202–1219; *Angew. Chem. Int. Ed.* **2008**, *47*, 1184–1201; c) A. Coskun, E. U. Akkaya, *J. Am. Chem. Soc.* **2006**, *128*, 14474–14475.
[34] M. J. Yuan, W. D. Zhou, X. F. Liu, M. Zhu, J. B. Li, X. D. Yin, H. Y. Zheng, Z. C. Zuo, C. Ouyang, H. B. Liu, Y. L. Li, D. B. Zhu, *J. Org. Chem.* **2008**, *73*, 5008–5014.
[35] Compound 4′-B-BODIPY was obtained from 4′-Br-BODIPY by treatment with pinacol ester of diboronic acid in the palladium-catalyzed reaction conditions according to the method reported by Suzuki: a) M. Sekiya, K. Umezawa, A. Sato, D. Citterio, K. Suzuki, *Chem. Commun.* **2009**, 3047–3049; 5′-Br-TMR was obtained according to Corrie's method: b) J. E. T. Corrie, J. S. Craik, *J. Chem. Soc. Perkin Trans. 1* **1994**, 2967–2973.
[36] J. W. Han, J. C. Castro, K. Burgess, *Tetrahedron Lett.* **2003**, *44*, 9359–9362.
[37] Y. K. Yang, K. J. Yook, J. Tae, *J. Am. Chem. Soc.* **2005**, *127*, 16760–16761.
[38] a) X. Q. Zhan, Z. H. Qian, H. Zheng, B. Y. Su, Z. Lan, J. G. Xu, *Chem. Commun.* **2008**, 1859–1861; b) W. Shi, H. M. Ma, *Chem. Commun.* **2008**, 1856–1858; c) X. Q. Chen, S. W. Nam, M. J. Jou, Y. Kim, S. J. Kim, S. Park, J. Yoon, *Org. Lett.* **2008**, *10*, 5235–5238.
[39] H. B. Yu, M. Y. Fu, Y. Xiao, *Phys. Chem. Chem. Phys.* **2010**, *12*, 7386–7391.
[40] a) K. K. Jensen, S. B. van Berlekom, J. Kajanus, J. Mårtensson, B. Albinsson, *J. Phys. Chem. A* **1997**, *101*, 2218–2220; b) K. Kilså, J. Kajanus, J. Mårtensson, B. Albinsson, *J. Phys. Chem. B* **1999**, *103*, 7329–7339.
[41] X. L. Zhang, Y. Xiao, X. H. Qian, *Org. Lett.* **2008**, *10*, 29–32.
[42] M. Fischer, J. Georges, *Chem. Phys. Lett.* **1996**, *260*, 115–118.
[43] a) I. Rosenthal, P. Peretz, K. A. Musrksf, *J. Phys. Chem.* **1979**, *83*, 350–353; b) D. A. Hinckley, P. G. Seybold, D. P. Borria, *Spectrochim. Acta A* **1986**, *42*, 747–754.
[44] F. H. Ko, L. Y. Weng, C. J. Ko, T. C. Chu, *Microelectron. Eng.* **2006**, *83*, 864–868.
[45] K. Helttunen, P. Prus, M. Luostarinen, M. Nissinen, *New J. Chem.* **2009**, *33*, 1148–1154.
[46] C. J. Stephenson, K. D. Shimizu, *Org. Biomol. Chem.* **2010**, *8*, 1027–1032.
[47] Y. K. Yang, H. J. Cho, J. Lee, I. Shin, J. Tae, *Org. Lett.* **2009**, *11*, 859–861.
[48] Y. K. Yang, S. K. Ko, I. Shin, J. Tae, *Org. Biomol. Chem.* **2009**, *7*, 4590–4593.
[49] E. M. Nolan, J. Jaworski, K. I. Okamoto, Y. Hayashi, M. Sheng, S. J. Lippard, *J. Am. Chem. Soc.* **2005**, *127*, 16812–16823.
[50] Z. X. Han, X. B. Zhang, L. Zhuo, Y. J. Gong, X. Y. Wu, J. Zhen, C. M. He, L. X. Jian, Z. Jing, G. L. Shen, R. Q. Yu, *Anal. Chem.* **2010**, *82*, 3108–3113.

Received: August 30, 2010
Published online: February 10, 2011

